A Parallel-Plate Flow Chamber to Study Initial Cell Adhesion on a Nanofeatured Surface

Elena Martines*, Kieran McGhee, Chris Wilkinson, and Adam Curtis

***Abstract*—Cells in the human body come across many types of information, which they respond to. Both material chemistry and topography of the surface where they adhere have an effect on cell shape, proliferation, migration, and gene expression. It is possible to create surfaces with topography at the nanometric scale to allow observation of cell-topography interactions. Previous work has shown that 100-nm-diameter pits on a 300-nm pitch can have a marked effect in reducing the adhesion of rat fibroblasts in static cultures. In the present study, a flow of cell suspension was used to investigate cell adhesion onto nanopits in dynamic conditions, by means of a parallel-plate flow chamber. A flow chamber with inner nanotopography has been designed, which allows real-time observation of the flow over the nanopits. A nanopitted pattern was successfully embossed into polymethylmethacrylate to meet the required shape of the chamber. Dynamic cell adhesion after 1 h has been quantified and compared on flat and nanopitted polymethylmethacrylate substrates. The nanopits were seen to be significantly less adhesive than the flat substrates ($p < 0.001$), which is coherent with previous observations of static cultures.**

***Index Terms*—Cell adhesion, embossing, flow, nanotopography, polymethylmethacrylate, topography**

I. Introduction

THE ADHESION of cells to their surroundings is of crucial importance in governing a range of cell functions in physiology, pathology, and biotechnological applications. Tissue engineers are interested in cell adhesion onto artificial biomaterials, since a better knowledge of cell behavior can be applied in clinical trials: there is a need for designing prosthetic devices whose surface triggers a specific cell response, e.g., giving control over the phenotype and activity of the cells, or reducing inflammation around the implant.

An important factor in cell adhesion is the shape of the surface ("topography") to which they adhere: different surface patterns have been shown to affect cell adhesion, morphology, and gene expression [1], [2].

By modifying the topography of surfaces, it is possible to study cell reaction to a variety of patterns. Surfaces with topographies at the micrometric [3], [4] and nanometric scale [5]–[9] can be created to allow observation of cell–surface interactions *in vitro*; it is interesting to investigate the implications of varying such a system, since the reaction of cells depends strongly on cell type and feature aspect ratio [2], [5], [8], [10]–[12].

The fabrication of nanopatterned substrates can be achieved with high-precision techniques like photolithography and electron beam lithography; both are used in-house. The electron beam lithography yields a lateral resolution as high as 5–10 nm, but unfortunately, although very precise, it is also expensive and time consuming, especially if large areas need to be patterned. To overcome these inconveniences, it is possible to replicate the substrate topography by embossing a mold into polymers, which also allows the combination of the topography with different materials in a cheap and reliable way [9], [13], [14].

Previous work has shown that 60–150-nm-diameter pits on a 300-nm pitch in polycaprolactone (PCL) can have a marked effect in reducing epitenon cell adhesion in static cultures [11], [15]. It is interesting to note that also some biological surfaces show functional nanometric patterns that prevent contamination and biofouling [16], [17].

The work of Gallagher *et al.* [15] was carried out in static conditions, where Brownian motion, gravity, and perhaps convection are the main acting forces. We wanted to build a system where hydrodynamic forces play the biggest role; the reason behind this is that cell adhesion under flow conditions has a very important role in many physiological functions, e.g., in the immune and developmental system. In the living body many cells are always surrounded or transported by actively moving fluids. Making cells flow onto a substrate can change their adhesion process, binding strength, and morphology with respect to a static culture [18]–[21]. Not only it is, perhaps, physiologically correct to culture cells in a flow, but it allows us to investigate phenomena (e.g., the rolling motion of leukocytes [22] or the migration of granulocytes [23]) whose mechanisms are still poorly understood. A number of flow chambers have been developed through the years, including parallel-plate flow chambers and stagnation-point flow chambers, that have been used to study, among others, cell adhesion, bacterial adhesion, microsphere deposition, and receptor–ligand bonds [18], [19], [21], [22], [24]–[28]; in a parallel-plate flow chamber, the motion of a sphere in laminar flow can be predicted with high approximation, and cell trajectories, speed, and adhesion can be monitored.

This study combines the use of a parallel-plate flow chamber and of nanopatterned polymethylmethacrylate surfaces: as a result, the cells flow steadily over nanopits 100 nm in diameter on a 300-nm pitch. This system allows observation and counting of cells, reproducibility of the experiment, and easy assembly of the nanotopography inside the chamber. Cell adhesion after 1-h flow was quantified.

Manuscript received March 2, 2004; revised March 15, 2004. This work was supported by the Engineering and Physical Sciences Research Council. *Asterisk indicates corresponding author.*

*E. Martines is with the Centre for Cell Engineering, Institute of Biomedical and Life Sciences, University of Glasgow, Glasgow G12 8QQ, U.K. (e-mail: elena@mblab.gla.ac.uk).

K. McGhee and C. Wilkinson are with the Department of Electronics and Electrical Engineering, University of Glasgow, Glasgow G12 8QQ, U.K.

A. Curtis is with the Centre for Cell Engineering, Institute of Biomedical and Life Sciences, University of Glasgow, Glasgow G12 8QQ, U.K.

Digital Object Identifier 10.1109/TNB.2004.828268

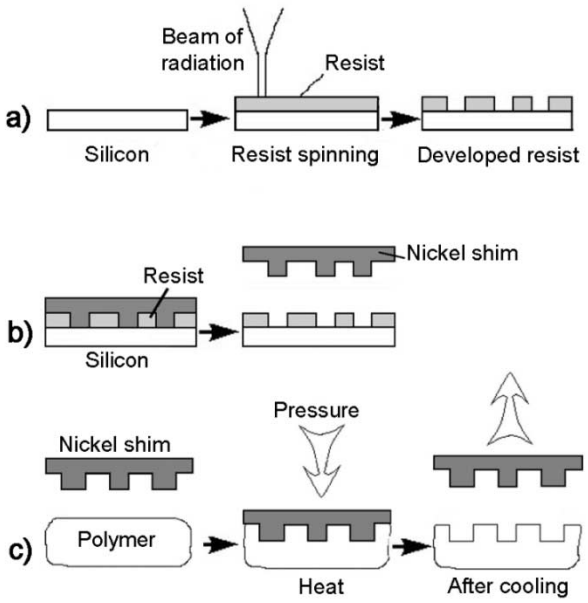

Fig. 1. Fabrication of nanopatterned PMMA. (a) Electron-beam lithographic process. (b) Electroplating. (c) Embossing of the nickel shim into the polymer.

II. Materials and Methods

A. Fabrication of the Substrate

Samples of polymethylmethacrylate (PMMA) (GoodFellow Cambridge Ltd., Huntingdon, U.K., 1-mm thickness) were patterned following three steps (Fig. 1).

1) The pitted pattern (100-nm-diameter pits on a 300-nm pitch) was written by electron beam lithography (Leica EBPG5-HR) in the resist onto a silicon master [15].
2) A nickel shim was electroplated on the developed resist [9]; thus, the shim was the mold which carried the negative image of the nanopatterned resist.
3) The nickel shim was embossed into a sheet of solid PMMA in an embossing machine (Nanoimprinter, Obducat, Malmö, Sweden). The pattern on the PMMA is the same as on the resist.

PMMA was chosen because of its biocompatibility and physical properties (transparent, suitable melting temperature). In the Nanoimprinter, the shim is pressed against the polymer, which is heated above its glass transition temperature (approximately 90 °C). The polymer flows in the nanocavities of the shim, and is then cooled (with an injected flow of cold nitrogen) and separated.

A square nanopitted pattern (15×15 mm^2) was embossed in the middle of rectangular PMMA sheets at 180 °C under 15 bars for 300 s; these samples were used as the bottom wall of the flow chambers (Fig. 2).

1) Observation of the Replicas: The embossed PMMA substrates were sputter coated with AuPd, then examined by a Hitachi S800 scanning electron microscope at a voltage of 10 keV.

B. Flow Chamber

The embossed PMMA substrates were sonicated in ethanol for 1 min and in Millipore water for 2 min, and then further rinsed in water twice. The glass slides were cleaned by sonicating in Opticlear, acetone, iso-propanol and water. A sheet of thermoplastic polymer (Nescofilm, Bando Chemical Ind. Ltd., Osaka, Japan) was cut (around a metal master) to create a waterproof gasket for the flow chamber. A parallel-plate flow chamber (Fig. 2) was constructed by clamping the thermoplastic gasket between a glass slide and the patterned PMMA substrate. The chamber was sealed by melting the gasket at 50 °C for 12 h using glass coverslips (0.17 mm thick) as spacers. Two circular holes in the glass slide provided the inlet and outlet of the flow. The chamber is designed to create a laminar flow over the substrate (see Appendix for calculations). The cells interacted with the PMMA topography on the lower wall of the chamber.

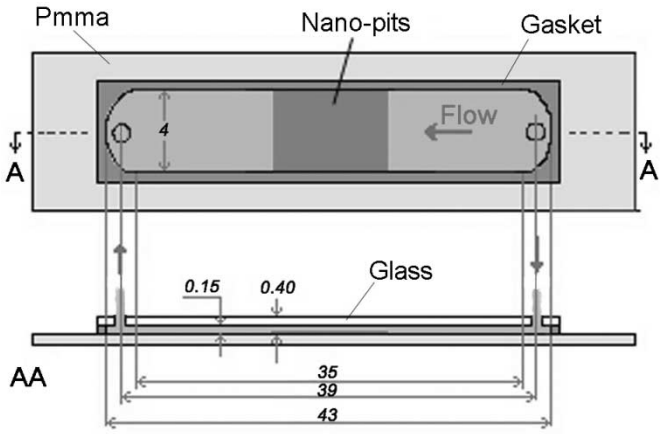

Fig. 2. Flow chamber (dimensions in millimeters).

C. Cell Culture

Rat epitenon fibroblasts were cultured from laboratory stocks (described by Wojciak *et al.* [29]) in HECT complete medium (hepes-buffered Glasgow-modified Eagle's medium (Biowest, Ringmer, East Sussex, U.K.) supplemented with 3% bicarbonate (Gibco, Paisley, U.K.), 10% calf serum (Gibco), 3% antibiotics (Gibco), 10% tryptose broth (Sigma, Dorset, U.K.), 2.85 mM glutamine). Before reaching confluence, the cells were rinsed with hepes/saline and detached for 3 min in 0.01% trypsin in versene. After addition of medium, centrifugation, and counting, a suspension of 10^6 cells/ml was prepared.

D. Flow Apparatus

The flow chamber was inserted in a flow cell, to which the pipes were connected (Fig. 3). A 5-ml syringe containing 3 ml of cell suspension generated the flow from a translational syringe-pump (CFP, Chesterfield, U.K.). The flow rate Q depends on the diameter of the syringe (the diameter of a 5-ml syringe is 11.12 mm) and on the translational velocity of the pump V_{syringe}. Table I shows the experimental conditions used for this study.

The flow reached the flow cell through polyvinyl chloride (PVC) pipes (of bore diameter 0.5 mm, Altec, Alton Hants, U.K.), then the inside of the chamber through the circular inlet. The flow chamber was rinsed with a flow of 70% ethanol for 10 min, Millipore water for 10 min, then with ECT growth medium (same as HECT, but not hepes-buffered) for 10 min.

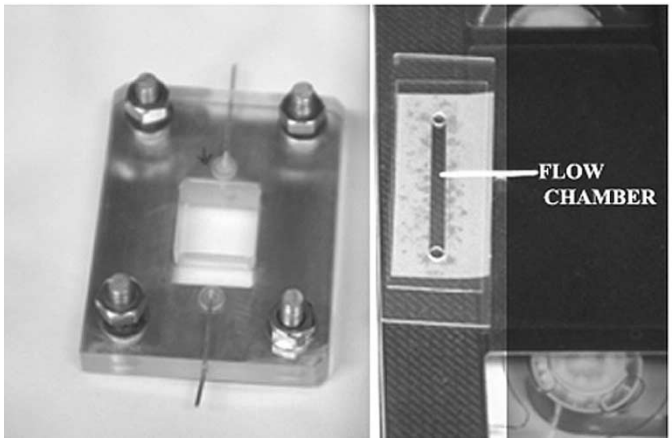

Fig. 3. Flow cell and flow chamber.

TABLE I
CHARACTERISTICS OF THE FLOW GENERATED BY A 5-ML SYRINGE AT THE PUMP SPEED V_{syringe} OF 1.32 μM/S

Dimensions (Lxbx2h)	35x4x0.17 mm^3
μ_{HECT} (viscosity)	$0.7734x10^{-3}$ N-s/m^2
ρ_{HECT} (density)	1.012 g/ml
γ_{wall} (shear rate)	7 s^{-1}
Re (Reynolds number)	0.02
l_e (entrance length)	0.6 μm

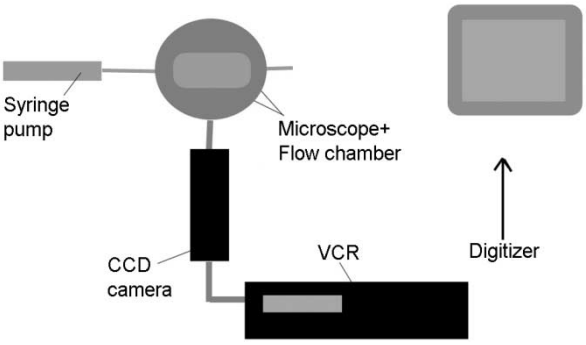

Fig. 4. Flow and recording apparatus.

The flow of suspended epitenon cells (10^6 cells/ml) in HECT medium was allowed for 1 h, then the chamber was rinsed with 4% formaldehyde in phosphate-buffered saline (PBS) for 15 min. The formalin fixed the cells that had adhered to the substrate, while washing off the others. When no free-flowing cells were visible, images were acquired for cell counting. All experiments were carried out at 37 °C. New PVC pipes and a new flow chamber were used at each experiment.

The chamber was observed under an inverted microscope (Leitz Diavert, Wetzlar, Germany). A charge-coupled device (CCD) camera (Panasonic VW-BL600) captured bright-field images with a 2.5 X objective, which were recorded on a Panasonic AG-6720A videorecorder and shown on a monitor (Fig. 4). Between 11 and 24 frames per experiment were acquired within a 15×4 mm^2 area (the visible patterned area) on four controls and six pitted substrates. The images were digitized with NIH Image (National Institute of Health, Washington, DC) and the adhering cells were counted manually; the cells gathering into clumps were counted as individual ones (Fig. 5).

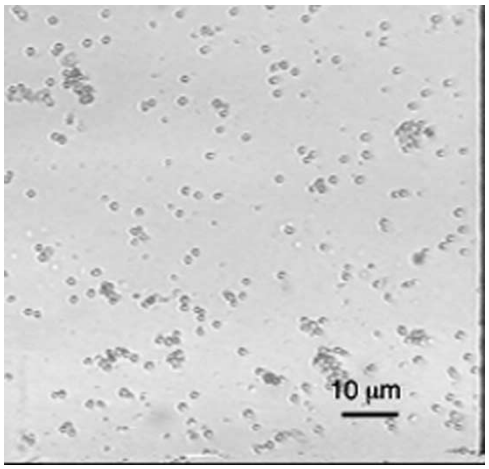

Fig. 5. Cells fixed in the flow chamber (after 1-h flow).

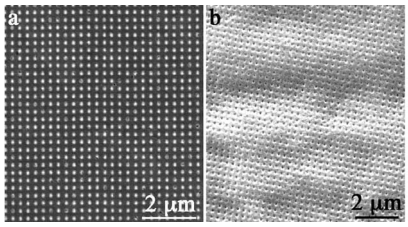

Fig. 6. Scanning electron microscopy images: (a) Nickel shim. (b) Nanopits embossed in PMMA.

Two-tailed t-test (assuming unequal variances) was used to compare the statistical significance of cell adhesion on the patterned substrates against the flat control.

III. RESULTS

Embossing was found to be a suitable technique to obtain transparent, thin sheets (approximately 1.2 mm) for the assembling of this flow chamber. Scanning electron microscopy showed that the nanopatterns were successfully embossed, reproducing the original topography of the resist (Fig. 6). The embossed PMMA samples are suitable for observation under a light microscope, since their transparency yields a very good image quality.

A flow chamber has been designed, which allows real-time, unobtrusive imaging of cells flowing onto a symmetrical nanopatterned substrate. The small height of the chamber makes sure that the flow is laminar and steady over the nanopits (see Appendix for more detail); in such a flow regime it is possible to quantify cell motion by measurements of cell trajectory and speed.

As far as cell adhesion is concerned, Fig. 7 shows the results yielded by this experiment. Epitenon cells adhere much less to the nanopits than to the flat controls. The t-test indicates that these results are statistically significant. Rolling motion and short-time arrests were observed, as reported by Pierres *et al.* [24]. Cell clumps formed on both patterned and flat surfaces, suggesting that cells adhere more easily to other cells rather than to the substrate, or simply that an adhered cell constitutes an obstacle for a flowing one, thus starting the nucleation of clumps (Fig. 5).

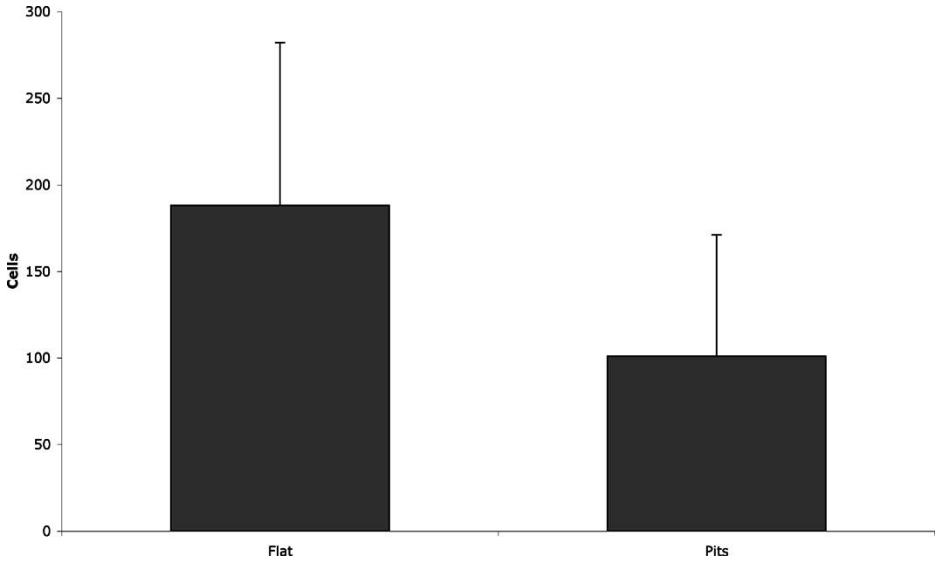

Fig. 7. Graphs of cell counts for epitenon cells on flat control $(1, n = 71)$ and nanopitted substrates $(2, n = 97)$. Results are mean ± standard deviation. Statistics by t-test $(p < 0.001)$.

IV. Discussion

By producing replicas it is possible to create a large number of inexpensive nanotopographies in a variety of polymers (PMMA, PCL, polycarbonate, etc.). PMMA proved to be the best option for this application, since its glass transition temperature is higher than the one required to seal the flow chamber. The nanopits were successfully embossed in the polymer. Other biocompatible materials should be tried in the future.

This flow chamber proved to be a reliable way of observing a cell flow. It is easily reproducible, cost effective, and of simple assemblage.

The next step in the system design involves the fabrication of a flow cell and chamber where only the patterned PMMA is replaced at each experiment, instead of the whole chamber. This would prevent the time-consuming problems encountered with leaking and/or stress concentration at the circular inlet.

Also, the whole system could be improved by the use of a different flow supply: although the flow can be kept for up to 14 h at a flow rate of 28 s^{-1}, the cells sediment in the syringe, which means that after approximately 1 h, only growth medium is flowing into the chamber. For this reason, only the initial adhesion was quantified. As a consequence, a morphological analysis of the adhered cells (i.e., quantification of cytoskeletal orientation, area, perimeter of the cells) is not possible because the adhered cells need at least 3 h to spread on the substrate.

Previous work has shown that some nanopatterned surfaces prevent or reduce static epitenon cell adhesion *in vitro* [15]. The purpose of the present study was to investigate cell adhesion on the nanopits, but in dynamic conditions, which is a much more physiological-resembling situation than the static culture. The present results showed again a significant effect of the nanopits in reducing cell adhesion, meaning that in the interplay of hydrodynamic and interfacial forces, the pattern has still a strong influence. It can be concluded that the cells can "sense" the nanotopography even when undergoing much stronger mechanical forces.

There are reasons to believe that the interfacial forces of some nanopitted surfaces are responsible for the cell adhesion changes, and different hypothesis have been made to explain this phenomenon [11], [30]. One of the most appealing explanations is that the changes in wettability induced by the pattern [31] selectively change the protein adsorption at the surface, thus affecting the formation of receptor–ligand bonds [30], [32]. Theoretical models could help understanding the change in interfacial energy that are caused by the surface topography; many attempts have been made to model the colloidal interactions between rough surfaces and micrometric spheres [33], [34]. Although these idealized systems do not compare directly to the cell–surface interactions, the case of convex asperities (dots) has been successfully addressed by Suresh *et al.* [33], suggesting that surface roughness might increase the attraction that causes the flocculation of particles. The case of hollow asperities (pits) has been treated by Herman *et al.* [34].

Our next experiment involves the variation of the flow speed to quantify initial cell adhesion on nanopits at different shear rates. Also, a morphological analysis of cells will be carried out by letting the flow run for longer times. Furthermore, since the reaction of cells to nanofeatures has been shown to be cell type dependent, it would be interesting to reproduce these experiments with other cell types; in particular, the behavior of human blood cells at physiological blood shears (>100 s^{-1} [37]) on nanotopography should be investigated.

Appendix

There are a very few known cases for which the equations of viscous flow can be solved without approximation; one of them is the flow of an incompressible fluid between two parallel infinite plates [38]. For this geometry the fluid particles move in the x direction parallel to the plates, and there is no velocity in the y and z direction (Fig. 8). In the case of steady flow, the Navier–Stokes equations are easily solved and, if the two plates are fixed, the velocity distribution becomes

$$u_x = \frac{1}{2\mu}\left(\frac{\partial p}{\partial x}\right)(y^2 - h^2) \tag{1}$$

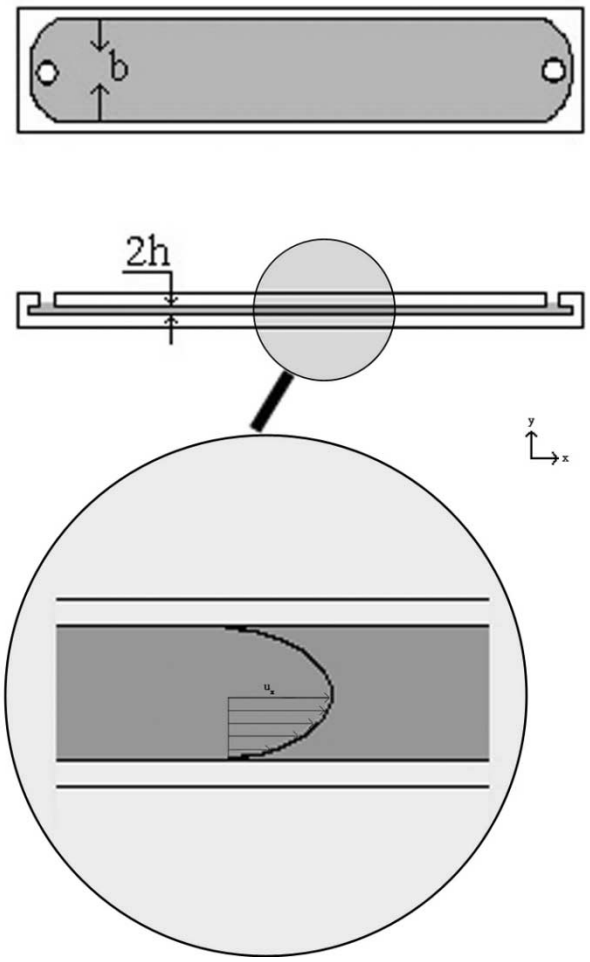

Fig. 8. The flow chamber in this project is a rectangular duct.

where μ is the dynamic viscosity of the fluid, p is the hydrodynamic pressure, and h is the half height of the chamber. Equation (1) shows that the velocity profile u_x between the two fixed plates is parabolic (Fig. 8), i.e., the flow is laminar (characterized by the "slipping motion of layers of fluid over other layers" [39]). In the case of rectangular ducts, such as the flow chamber in this project, the equations cannot so easily be solved, and the solution is more complex [40]. Because of two pair of sidewalls, the velocity profile is a paraboloid.

However, in this chamber the width b is 23 times greater than the height h, so that the two slides have been considered as two infinite (wide) parallel plates. The flow is also assumed to be steady and incompressible, and the fluid Newtonian. For this model, three parameters have been calculated (Table I): 1) the Reynolds number (Re); 2) the entrance length l_e; and 3) the wall shear rate γ_{wall}.

A. Reynolds Number

A way to predict if the flow is going to be laminar or not is to calculate the dimensionless Re, which is the ratio between the inertial forces and the viscous forces due to the flow (2). If $\text{Re} \ll 1$, the viscous forces are predominant, so the flow will be laminar

$$\text{Re} = \frac{\rho V D}{\mu} \tag{2}$$

$$D = \frac{4bh}{b+2h} \tag{3}$$

where (3) is the hydraulic diameter for rectangular pipes [38], ρ is the density of the fluid, V is the mean velocity of the flow, h is half the height of the chamber, and b is the width of the chamber.

The dynamic viscosity μ of the suspension can be calculated as to Happel and Brenner [41], and in the case of our dilute system, it can be approximated to the viscosity of the HECT medium, which has been measured with a 27 942 ASTM-IP Ostwald viscometer. At 37 °C

$$\rho_{\text{HECT}} = 1.012\ \text{g/ml}$$
$$\mu_{\text{HECT}} = 0.7734 \times 10^{-3}\ N - s/m^2.$$

Calculations of Re for this flow chamber show that the viscous effects are predominant $(\text{Re} = 0.02)$, which is not surprising due to the small height of the chamber.

B. Entrance Length

When the flow is entering the chamber, it needs a certain length before it becomes fully developed, i.e., before the velocity profile becomes parabolic. This is the so-called entrance length l_e. Different correlations have been accepted to calculate the entrance length [38], [39]; for this chamber, [38, eq. (4)] has been used, where D is the hydraulic diameter:

$$l_e = 0.065\,\text{Re}\,D. \tag{4}$$

The turbulent effects due to the geometry have not been considered (the flow pattern represents a sharp-edged "source and sink" configuration [39]), which means that the entrance length is longer than calculated. However, the distance between the inlet and the centre of the chamber is 19.5 mm, which is 10^4 times bigger that the calculated entrance length ($l_e = 0.6\ \mu$m): it seems, then, reasonable to assume that the flow in the middle is fully developed.

C. Wall Shear Rate

The most commonly cited hemodynamic factor implicated in cell adhesion defects, disease initiation, and ligand-receptor bond dissociation is the wall shear stress τ_{wall}, while the wall shear rate $\gamma_{\text{wall}} (= \tau_{\text{wall}}/\mu)$ seems to affect bond formation [42]. The shear rate γ quantifies the speed of deformation of a flowing fluid, and it is inversely proportional to the viscosity μ. The wall shear rate is calculated from the velocity distribution in a Newtonian fluid flowing between two wide, parallel plates [38] (5)

$$\gamma_{\text{wall}} = \frac{3Q}{2bh^2} \tag{5}$$

where Q is the flow rate. In this flow chamber, $\gamma_{\text{wall}} = 7\ \text{s}^{-1}$.

Acknowledgment

The authors would like to thank Dr. N. Gadegaard, Dr. M. Riehle and Prof. H. Morgan for discussion, and Mr. A. McGregor, Mr. G. Baxter (IBLS Mechanical Workshop,

Glasgow, U.K.), and Mr. K. Piechowiak (Electronics Mechanical Workshop, Glasgow, U.K.) for technical assistance.

REFERENCES

[1] A. Curtis and C. D. W. Wilkinson, "Topographical control of cells," *Biomaterials*, vol. 18, pp. 1573–1583, 1997.

[2] M. Dalby, S. J. Yarwood, M. O. Riehle, H. J. H. Johnstone, S. Affrossman, and A. S. G. Curtis, "Increasing fibroblast response to materials using nanotopography: Morphological and genetic measurements of cell response to 13-nm-high polymer demixed islands," *Exp. Cell Res.*, vol. 276, pp. 1–9, 2002.

[3] B. Chehroudi and D. M. Brunette, "Effects of surface topography on cell behavior," in *Encyclopedic Handbook of Biomaterials and Bioengineering. Part S: Materials*, D. Donald, L. Wise, D. E. Altobelli, M. J. Yaszenski, J. D. Gresser, and E. R. Schwartz, Eds. New York: Marcel Dekker, 1995.

[4] D. L. Rovenski YA, O. Y. Ivanova, and J. M. Vasiliev, "Locomotory behavior of epitheliocytes and fibroblasts on metallic grids," *J. Cell Sci.*, vol. 112, pp. 1273–1282, 1999.

[5] P. Clark, P. Connolly, A. S. G. Curtis, J. A. T. Dow, and C. D. W. Wilkinson, "Cell guidance by ultrafine topography *in vitro*," *J. Cell Sci.*, vol. 99, pp. 73–77, 1991.

[6] C. Wilkinson, M. Riehle, M. A. Wood, J. O. Gallagher, and A. S. G. Curtis, "The use of materials patterned on a nano- and micro-metric scale in cellular engineering," *Mater. Sci. Eng.*, 2001.

[7] M. Dalby, M. O. Riehle, S. Affrossman, and A. S. G. Curtis, "In vitro reaction of endothelial cells to polymer demixed nanotopography," *Biomaterials*, vol. 23, pp. 2945–2954, 2002.

[8] C. Wilkinson, A. S. G. Curtis, and J. Crossan, "Nanofabrication in cellular engineering," *J. Vac. Sci. Tech. B*, vol. 16, pp. 3132–3136, 1998.

[9] N. Gadegaard, S. Thoms, D. S. Macintyre, K. Mcghee, J. O. Gallagher, B. Casey, and C. D. W. Wilkinson, "Arrays of nano-dots for cellular engineering," *Microelectron. Eng.*, vol. 67–68, pp. 162–168, 2003.

[10] A. Curtis and C. D. W. Wilkinson, "Topographical control of cell migration," in *Motion Analysis of Living Cells, Techniques in Modern Biomedical Microscopy*, D. Soll and D. Wessels, Eds. New York: Wiley-Liss, 1998, pp. 141–156.

[11] A. Curtis, B. Casey, J. O. Gallagher, D. Pasqui, M. A. Wood, and C. D. W. Wilkinson, "Substratum nanotopography and the adhesion of biological cells. Are symmetry or regularity of nanotopography important?," *Biophys. Chem.*, vol. 94, pp. 275–283, 2001.

[12] M. Riehle, "Cell behavior of rat calvaria bone cells on surfaces with random nanometric features," *Mater. Sci. Eng. C*, vol. 23, pp. 337–340, 2003.

[13] Y. Xia, J. A. Rogers, K. E. Paul, and G. M. Whitesides, "Unconventional methods for fabricating and patterning nanostructures," *Chem. Rev.*, vol. 99, pp. 1823–1848, 1999.

[14] L. Heyderman, H. Schift, C. David, J. Gobrecht, and T. Shweizer, "Flow behavior of thin polymer films used for hot embossing lithography," *Microelectron. Eng.*, vol. 54, pp. 229–245, 2000.

[15] J. O. Gallagher, K. F. McGhee, C. D. W. Wilkinson, and M. O. Riehle, "Interaction of animal cells with ordered nanotopography," *IEEE Trans. Nanobiosci.*, vol. 1, pp. 24–28, Mar. 2002.

[16] W. Barthloot and C. Neinhuis, "Purity of the sacred lotus, or escape from contamination in biological surfaces," *Planta*, vol. 202, pp. 1–8, 1997.

[17] C. Baum, W. Meyer, R. Stelzer, L. G. Fleisher, and D. Siebers, "Average nanorough skin surface of the pilot whale (globicephala melas, delphinidae): Considerations on the self-cleaning abilities based on nanoroughness," *Marine Biol. Online*, 2001.

[18] P. Bongrand, P. M. Claesson, and A. S. G. Curtis, *Studying Cell Adhesion*. Heidelberg, Germany: Springer-Verlag, 1994.

[19] J. Doroszewski, J. Skierski, and L. Przadka, "Interaction of neoplastic cells with glass surface under flow conditions," *Exp. Cell Res.*, vol. 104, pp. 335–343, 1977.

[20] T. Van Kooten, J. M. Schakenraad, H. C. Van der Mei, and H. J. Busscher, "Development and use of a parallel-plate flow chamber for studying cellular adhesion to solid surfaces," *J. Biomed. Mater. Res.*, vol. 26, pp. 725–738, 1992.

[21] M. Stavridi, M. Katsikogianni, and Y. F. Missirlis, "The influence of surface patterning and/or sterilization on the heamocompatibility of polycaprolactones," *Mater. Sci. Eng. C*, vol. 23, pp. 359–365, 2003.

[22] O. Tissot, A. Pierres, C. Foa, M. Delaage, and P. Bongrand, "Motion of cells sedimenting on a solid surface in a laminar shear flow," *Biophys. J.*, vol. 61, pp. 204–215, 1992.

[23] J. Doroszewski and A. Kiwala, "Adhesion and locomotion of granulocytes under flow conditions," *J. Cell Sci.*, vol. 90, pp. 335–340, 1988.

[24] A. Pierres, A. M. Benoliel, and P. Bongrand, "Measuring bonds between surface-associated molecules," *J. Immunol. Methods*, vol. 196, pp. 105–120, 1996.

[25] R. Poyton and D. Branton, "A multipurpose microperfusion chamber," *Exp. Cell Res.*, vol. 60, pp. 109–114, 1970.

[26] J. Dvorak and W. Stotler, "A controlled-environment culture system for high resolution light microscopy," *Exp. Cell Res.*, vol. 68, pp. 144–148, 1971.

[27] K. Spring and A. Hope, "Size and shape of the lateral intercellular spaces in a living epithelium," *Science*, vol. 200, pp. 54–57, 1978.

[28] J. Yang, R. Bos, A. Poortinga, P. J. Wit, G. F. Belder, and H. J. Busscher, "Comparison of particle deposition in a parallel plate flow chamber and a stagnation point flow chamber," *Langmuir*, vol. 15, pp. 4671–4677, 1999.

[29] B. Wojciak, J. Crossan, A. S. G. Curtis, and C. D. W. Wilkinson, "Grooved substrata facilitate In vitro healing of completely divided flexor tendons," *J. Mater. Sci.: Mater. Med.*, vol. 6, pp. 266–271, 1995.

[30] T. Webster, C. Ergun, R. H. Doremus, R. W. Siegel, and R. Bizios, "Specific proteins mediate enhanced osteoblast adhesion on nanophase ceramics," *J. Biomed. Mater. Res.*, vol. 51, pp. 475–483, 2000.

[31] J. Bico, C. Tordeux, and D. Quere, "Rough wetting," *Europhys. Lett.*, vol. 55, pp. 214–220, 2001.

[32] T. Ruardy, H. E. Moorlag, J. M. Schakenraad, H. C. Van der Mei, and H. J. Busscher, "Growth of fibroblasts and endothelial cells on wettability gradient surfaces," *J. Colloid Interface Sci.*, vol. 188, pp. 209–217, 1997.

[33] L. Suresh and J. Y. Walz, "Effect of surface roughness on the interaction energy between a colloidal sphere and a flat plate," *J. Colloid Interface Sci.*, vol. 183, pp. 199–213, 1996.

[34] M. Herman and K. D. Papadopoulos, "A method for modeling the interactions of parallel flat plate systems with surface features," *J. Colloid Interface Sci.*, vol. 142, pp. 331–342, 1991.

[35] W. Bowen and A. O. Sharif, "Hydrodynamic and colloidal interactions effects on the rejection of a particle larger than a pore in microfiltration and ultrafiltration membranes," *Chem. Eng. Sci.*, vol. 53, pp. 879–890, 1998.

[36] E. Kokkoli and C. F. Zokoski, "Surface pattern recognition by a colloidal particle," *Langmuir*, vol. 17, pp. 369–376, 2001.

[37] A. Hoeks, S. K. Samijo, P. J. Brands, and R. S. Reneman, "Noninvasive determination of shear-rate distribution across the arterial lumen," *Hypertension*, vol. 26, pp. 26–33, 1995.

[38] B. Munson, D. F. Young, and T. H. Okiishi, *Fundamentals of Fluid Mechanics*, 3rd ed. New York: Wiley, 1990.

[39] L. Prandtl, *Essentials of Fluid Dynamics*. London, U.K.: Blackie, 1952.

[40] W. Langlois, *Slow Viscous Flow*. New York: Macmillan, 1964.

[41] J. Happel and H. Brenner, *Low Reynolds Number Hydrodynamics*. New York: Prentice-Hall, 1965.

[42] S. Chen and T. A. Springer, "Selectin receptor–ligand bonds: Formation limited by shear rate and dissociation governed by the Bell model," *Proc. Nat. Acad. Sci.*, vol. 98, no. 3, pp. 950–955, Jan. 30, 2001.

Elena Martines received the M.Eng. degree from the Institut National des Sciences Appliquées (INSA), Lyon, France, in 2001. She is currently working toward the Ph.D. degree in the Centre for Cell Engineering, University of Glasgow, Galsgow, U.K.

Her research interests include the use of nanotopographic surfaces to study cell adhesion, microfluidic systems, and surface forces modeling.

Kieran McGhee, photograph and biography not available at the time of publication.

Chris Wilkinson, photograph and biography not available at the time of publication.

Adam Curtis, photograph and biography not available at the time of publication.